



**HAL**  
open science

## Microsphere structure application for supercapacitor in situ temperature monitoring

Paulina Listewnik, Mikhael Bechelany, Malgorzata Szczerska

► **To cite this version:**

Paulina Listewnik, Mikhael Bechelany, Malgorzata Szczerska. Microsphere structure application for supercapacitor in situ temperature monitoring. *Smart Materials and Structures*, 2021, 30 (10), pp.10LT01. 10.1088/1361-665X/ac221b . hal-03860465

**HAL Id: hal-03860465**

**<https://hal.umontpellier.fr/hal-03860465v1>**

Submitted on 2 Dec 2022

**HAL** is a multi-disciplinary open access archive for the deposit and dissemination of scientific research documents, whether they are published or not. The documents may come from teaching and research institutions in France or abroad, or from public or private research centers.

L'archive ouverte pluridisciplinaire **HAL**, est destinée au dépôt et à la diffusion de documents scientifiques de niveau recherche, publiés ou non, émanant des établissements d'enseignement et de recherche français ou étrangers, des laboratoires publics ou privés.

# Microsphere Structure Application for Supercapacitor *In Situ* Temperature Monitoring

Paulina Listewnik<sup>1</sup>, Mikhael Bechelany<sup>2</sup> and Małgorzata Szczerska<sup>1</sup>

<sup>1</sup> Department of Metrology and Optoelectronics, Faculty of Electronics, Telecommunications and Informatics, Gdańsk University of Technology, 11/12 Narutowicza Street, 80-233 Gdańsk, Poland

<sup>2</sup> Institut Européen des Membranes, IEM – UMR 5635, ENSCM, CNRS, Univ Montpellier, Montpellier, France

E-mail: malszcze@pg.edu.pl (MS)

Received 2 June 2021, revised 17 August 2021

Accepted for publication 26 August 2021

Published xxxxxx

## Abstract

Constant, real-time temperature monitoring of the supercapacitors for efficient energy usage is in high demand and seems to be crucial for further development of those elements. A fiber-optic sensor can be an effective optoelectronic device dedicated for in-situ temperature monitoring of supercapacitors. In this work, the application of the fiber-optic microstructure with thin zinc oxide (ZnO) coating fabricated in the atomic layer deposition process (ALD) applied as a temperature sensor is reported. Such a structure was integrated with supercapacitors and used for the temperature measurements. Described sensors are built with the utility of the standard optical telecommunication fibers. The inner temperature of the supercapacitor was investigated in the range extending from 30°C to 90°C with a resolution equal to 5°C. The sensitivity of temperature measurement is about 109.6 nW/°C. The fitting of the sensor was achieved with a correlation coefficient  $R^2 = 0.97$ .

Keywords: fiber-optic microstructure; fiber-optic microsphere; supercapacitor; fiber-optic sensor; temperature monitoring.

---

## 1. Introduction

Supercapacitors are designed as devices able to store substantially more amounts of energy than electrolytic capacitors [1]. Their many advantages, including high-power density, cyclic stability and durability, make supercapacitors highly sought-after storage devices, whether for standalone or hybrid applications [2,3].

Increasing demand for portable energy sources, supercapacitors are gaining more and more interest. Therefore, the possibilities of advancements of this technology are constantly investigated and new solutions are developed [4–7]. Learning about the inner workings of every device leads to gaining understanding of the processes occurring inside the device, which in turn allows to enhance their performance.

Real-time monitoring of the supercapacitor's internal temperature ensures efficient operation of the device. Temperature exceeding beyond the expected range is a good indicator of a faulty device. Whereas some changes can be undone, most are irreversible and contribute to the degradation of the device. Exceeding a limit beyond operating temperature can cause destabilization of electrolyte, which leads to further damage of supercapacitors. The electrolyte is a crucial component of any electrochemical electric cells, including supercapacitors [8–10]. Their purpose is to transfer charge between electrodes during electrochemical processes [11]. Parameters of the supercapacitors, such as power density, longevity, charging-discharging rates are largely dependent on their state, balance and conformity [12]. Overheating can cause the emergence of chemical reactions between the electrolyte and the

electrodes, and chemical decomposition which in turn impedes its performance, e.g., accelerate its aging, slow down charging cycles and speed up discharging cycles, distortion or even a rupture of the device [13–15]. On the other hand, extreme low-temperature performance is also damaging the device – it can cause increased charge transfer resistance or deteriorate electrodes and their contact with electrolyte [16,17].

Many factors can influence temperature distribution within the device, including elements of which supercapacitors are composed (electrode materials [18–21], charge storage mechanism [22,23], electrolyte) as well as its intended application or mode of operation [2,24]. However, in-situ monitoring of the device can often provide a better comprehension of the conditions occurring inside.

The distribution of the temperature in the pouch cells is widely studied to estimate the best construction of the device and to improve its efficiency. Starting with modelling and creating new algorithms as it is presented by Zhang et al. in [25] or by Wu et al. in [26]. The pouch cells are then investigated in experimental settings, using whether contactless methods like infrared thermography [27,28] or more direct methods such as measurements by thermocouples [29,30] and interferometric sensors [31,32]. However, none of the presented solutions provides additional information about the correct operation of the sensor at all times. To investigate the changes occurring in the supercapacitors, a fiber-optic sensors functionalized with a ZnO coating, similar to those presented in [33] and [34], can be utilized.

In this paper, an in-situ measurement of the temperature of the supercapacitor is presented. To accomplish it, a microsphere-based fiber-optic sensor with a 200 nm ZnO ALD coating was embedded in the device. With the use of the presented sensor, it is possible to simultaneously monitor the internal temperature of the supercapacitor and the integrity of the sensor head structure in real-time, therefore avoiding uncertainties resulting from faulty sensors. The research presented in this paper is an incremental advancement of a similar type of sensor. The application presented herein is unique due to the use of fiber optics for precise temperature measurement of supercapacitors, which is important because other methods cause variations in the electromagnetic field and disrupt the operation of the supercapacitors. In presented research ZnO coating is used as a sensing medium itself. And what we used is the dependence of the optical parameters on temperature. Furthermore, we use unusual for ALD technique thickness, which is very thick – 200 nm. Previously, dependence of the changing of the refractive index on the intensity of the reflected signal was measured using similar technique [35,36]. Furthermore, a validation of the microsphere-based temperature sensor is presented in [37].

## 2. Materials and Methods

The microsphere-based fiber-optic sensor with a 200 nm ZnO ALD coating was embedded inside the supercapacitor, in a manner to prevent disruption of its operation. The supercapacitors utilized in this research, their construction and parameters are described elsewhere [38]. The sensor was placed between the electrode and the foil forming the cover of the device. The location of the sensor inside the supercapacitor is presented in the schematic of the device's cross-section (Fig. 1.).

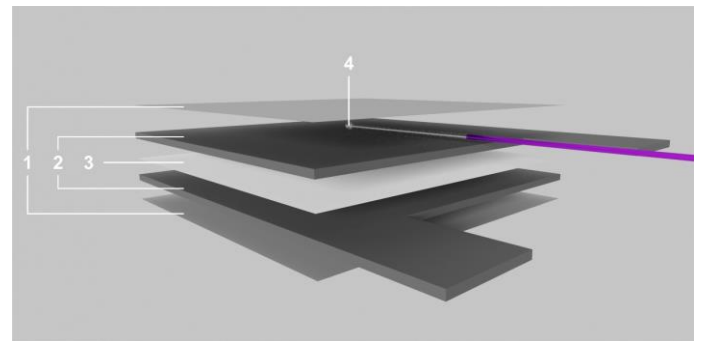


**Figure 1.** Placement of the microsphere-based fiber-optic sensor embedded in the supercapacitor in schematic cross-section where: 1 – covers, 2 - electrodes, 3 – separator, 4 – microsphere-based fiber-optic sensor.

The microsphere structure of the sensor was made at the tip of a standard telecommunication optical fiber (SMF-28, Thorlabs Inc., Newton, NJ, USA), using a fusion splicer (FSU975, Ericsson, Sweden). The obtained microsphere of the diameter of 245  $\mu\text{m}$  was formed during the three-step pull process. The image of the microstructure, obtained under a microscope (CX31, Olympus, Japan) is presented in Figure 2.



**Figure 2.** A microscope image of the microstructure used for supercapacitor in situ temperature measurement.

The sensor was used to observe changes in an optical spectrum while increasing the temperature of the device, and subsequent temperature growth of the electrolyte of which the investigated supercapacitors are composed. The device was tested in the temperature range of 30-90°C because of the aqueous properties of the used electrolyte (1 M K<sub>2</sub>SO<sub>4</sub>). While increasing the temperature, the electrolyte can change its properties, e.g., refractive index. More thorough research regarding refractive index sensing is presented in [35,36].

The supercapacitors were investigated using an interferometric setup consisting of a broad band light source with a central wavelength of 1310 ±10 nm (SLD-1310-18-W, FiberLabs Inc., Fujimi) which generates an optical signal. The experimental setup used for measurements of the supercapacitor's inner temperature is presented in Fig. 3.

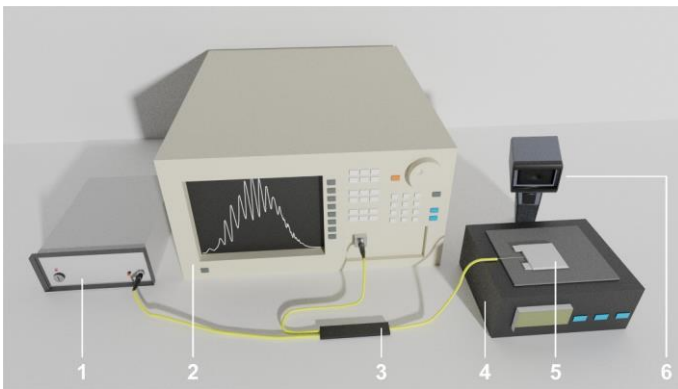


**Figure 3.** Measurement setup where: 1 – broadband light source, 2 – Optical Spectrum Analyzer, 3 – optical coupler, 4 – hot plate, 5 – investigated supercapacitor, 6 – thermal camera.

The signal is propagated through the optical coupler (G657A, CELLCO, Kobylanka, Poland) to the microsphere-based fiber-optic sensor where the phenomenon of interference is incited. The signal is reflected off the two boundaries from which the sensor is built. Firstly, a part of the signal reflects on the boundary between the inner sphere, made of the core of the fiber, and the outer sphere, made of the cladding of the fiber, while the rest is transmitted through and reaches the boundary between the outer sphere and the measured medium, on which it is also reflected. The two waves superpose, resulting in an interference effect. The placement of the sensor in the supercapacitor as well as its operation principle is presented in Fig. 4. When the temperature changes the optical parameters of the ZnO cladding such as refractive index change what influences the reflection coefficient of the second boundary and influences the phase differences between interfering beams.

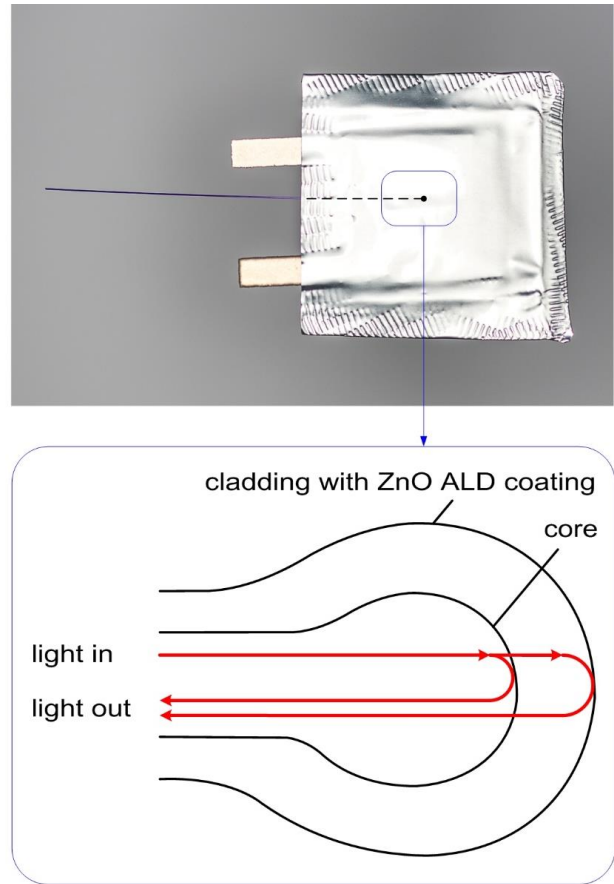


**Figure 4.** Operation principle of the in-situ fiber-optic sensor temperature monitoring.

The obtained signal is gathered by the Optical Spectrum Analyzer (OSA, Ando AQ6319, Yokohama, Japan). The data is then processed. The response time of the sensor is dependent on multiple factors, e.g., the type of utilized detector. The utilized OSA allows to read the data every 3 s. Preliminary measurements to determine the proper operation of the sensor and the results are presented in [37].

Throughout the measurements, the temperature of investigated supercapacitors was also verified by a thermal camera (i7, FLIR, Wilsonville, OR, USA) to ensure uniform distribution of the temperature. Images obtained from this test are presented in Fig. 5.

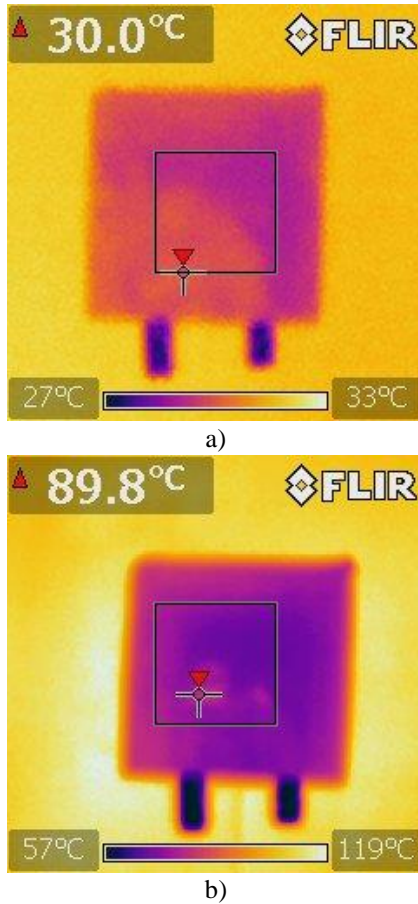


**Figure 5.** Images of the supercapacitor with the in-situ fiber-optic temperature sensor obtained by a thermal camera for the lowest a) 30°C and highest b) 89.8°C value of investigated temperature range.

The emissivity of the thermal camera was set to  $\epsilon=0.6$  during the measurements due to the fact that the supercapacitor has been enclosed in a triplex foil which reflectance value was taken into consideration during the measurements. The camera was set to measure the highest temperature inside the selected area and it is determined by the marker. Obtained measurement is presented in the top left corner of each image.

### 3. Results and discussion

This section discusses the data acquired during measurements performed in the experimental setup. All measurements were performed at least 5 minutes after stabilization of the temperature, which was controlled by observation through a thermal camera, while the supercapacitor's state of charge was at about 80%. Fig. 6 shows the changes in the spectrum while the temperature was growing in the set range.

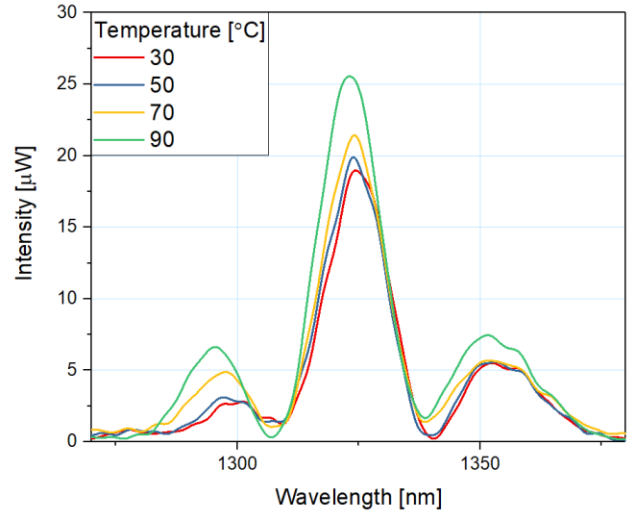


**Figure 6.** Changes in the intensity of the reflected signal with rising temperature.

As can be observed, the intensity of the reflected signal is increasing with the rise of temperature while the envelope retains similar. Moreover, the interference signal ensures that the sensor is not damaged. To maintain the clarity of the graph, only selected spectra were plotted. The dependence of the peak intensity of the reflected signal on the temperature is presented in Fig. 7.

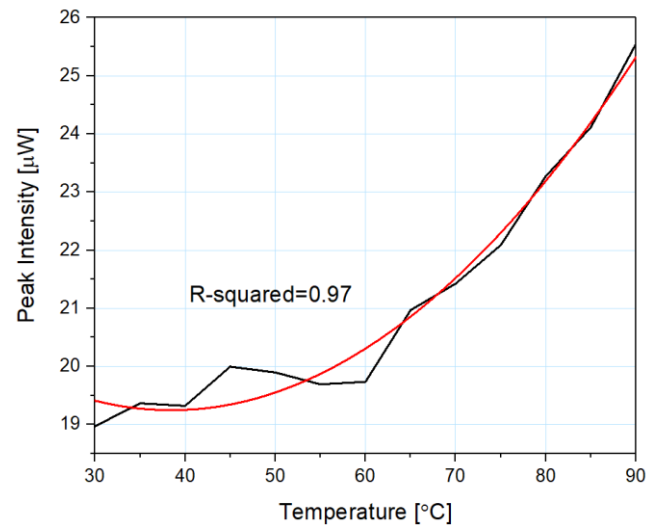


**Figure 7.** Reflected signal peak intensity dependence in the changing temperature.

Peak intensity increases according to the second-order polynomial fit. By including polynomial regression in Fig. 7, a match between obtained data and theoretical fitting can be estimated.  $R^2$  coefficient, which equals 0.97, exhibits a close fit of both plots. Based on the obtained data, the sensitivity of the sensor was calculated to be 109.6 nW/°C. Even though the sensitivity in the temperature range of 30-65°C is visibly lower (57 nW/°C), this behavior is repeatable throughout multiple measurement series, therefore it serves during the

monitoring of the internal temperature as a sensing mechanism. Having reference spectral characteristics of the healthy device, any deviation from the known will be noticeable indicating either warning or critical state.

Performed investigation shows that by embedding a microsphere-based fiber-optic sensor, the internal temperature of supercapacitors can be monitored. The obtained interferometric signal remains present, therefore indicating proper operation of the device. Upon the sensor sustaining the damage, the interference within the signal ceases. Furthermore, based on polynomial regression, the behavior of the characteristics can be estimated. Substantial deviation of the characteristic from the reference indicates that the investigated supercapacitor became defective. The information allows taking the steps to preserve the device.

#### 4. Conclusions

In this paper, the application of the microsphere-based fiber-optic sensor for in-situ monitoring of the temperature of the supercapacitor was examined. Because of a growing need for more efficient energy, it is necessary to thoroughly explore the processes occurring in the devices. The knowledge allows to optimize, find new solutions and improve current technology. The presented sensor was embedded inside the supercapacitor with aqueous electrolyte. During the operation of the device, we were able to investigate the in-situ temperature of the supercapacitor in a range of 30-90°C, with a resolution of 5°C, by observing changing optical spectrum. The intensity of the reflected signal increased, with the rise of the temperature and the presence of the interference indicated the integrity of the sensor, which in turn allowed to ensure the accuracy of the measurements. Based on the obtained data, the sensitivity of the sensor was calculated and it equals 109.6 nW/°C for the measured range. Thermal imaging was also performed to verify the accuracy of the measured temperature. The presented approach of internal temperature monitoring is ready to be used for application in the supercapacitors. Unlike other methods, it allows to constantly control the validity of performed measurements which is especially important in the devices and conditions where the inspection of the system operation and its components may not be feasible or easily reachable.

**Author Contributions:** Conceptualization, P.L. and M.S.; methodology, P.L. and M.S.; validation, P.L. and M.S.; formal analysis, P.L. and M.S.; investigation, P.L. and M.S.; resources, M.B.; data curation, P.L.; writing—original draft preparation, P.L.; writing—review and editing, M.S. and M.B.; visualization, P.L.; supervision, M.S.; project administration, M.S.; funding acquisition, M.S. All authors have read and agreed to the published version of the manuscript.

**Funding:** Financial support of these studies from Gdańsk University of Technology by the 8/2020/IDUB/III.4.1/Tc grant under the Technetium - EIRU program is gratefully acknowledged. The authors P.L. and M.S. acknowledge financial support of DS Programs of the Faculty of Electronics, Telecommunications and Informatics of the Gdańsk University of Technology.

**Informed Consent Statement:** Not applicable.

**Data Availability Statement:** 10.34808/pnwz-7035.

**Conflicts of Interest:** The authors declare no conflict of interest.

#### References

- [1] Frackowiak E 2007 Carbon materials for supercapacitor application *Phys. Chem. Chem. Phys.* **9** 1774
- [2] Raza W, Ali F, Raza N, Luo Y, Kim K-H, Yang J, Kumar S, Mehmood A and Kwon E E 2018 Recent advancements in supercapacitor technology *Nano Energy* **52** 441–73
- [3] Zhang L, Hu X, Wang Z, Sun F and Dorrell D G 2018 A review of supercapacitor modeling, estimation, and applications: A control/management perspective *Renewable and Sustainable Energy Reviews* **81** 1868–78
- [4] Wu Z-K, Lin Z, Li L, Song B, Moon K, Bai S-L and Wong C-P 2014 Flexible micro-supercapacitor based on in-situ assembled graphene on metal template at room temperature *Nano Energy* **10** 222–8
- [5] Naoi K, Naoi W, Aoyagi S, Miyamoto J and Kamino T 2013 New Generation “Nanohybrid Supercapacitor” *Acc. Chem. Res.* **46** 1075–83
- [6] Zuo W, Li R, Zhou C, Li Y, Xia J and Liu J 2017 Battery-Supercapacitor Hybrid Devices: Recent Progress and Future Prospects *Advanced Science* **4** 1600539
- [7] Najib S and Erdem E 2019 Current progress achieved in novel materials for supercapacitor electrodes: mini review *Nanoscale Advances* **1** 2817–27
- [8] Frackowiak E, Meller M, Menzel J, Gastol D and Fic K 2014 Redox-active electrolyte for supercapacitor application *Faraday Discuss.* **172** 179–98
- [9] Wu J, Yu H, Fan L, Luo G, Lin J and Huang M 2012 A simple and high-effective electrolyte mediated with p-phenylenediamine for supercapacitor *J. Mater. Chem.* **22** 19025–30
- [10] Liu X, Wu D, Wang H and Wang Q 2014 Self-Recovering Tough Gel Electrolyte with Adjustable Supercapacitor Performance *Advanced Materials* **26** 4370–5
- [11] Pal B, Yang S, Ramesh S, Thangadurai V and Jose R 2019 Electrolyte selection for supercapacitive devices: a critical review *Nanoscale Adv.* **1** 3807–35

- [12] Deng J, Li J, Song S, Zhou Y and Li L 2020 Electrolyte-Dependent Supercapacitor Performance on Nitrogen-Doped Porous Bio-Carbon from Gelatin *Nanomaterials* **10** 353
- [13] Yang H 2020 Effects of Aging and Temperature on Supercapacitor Charge Capacity 2020 *IEEE Power Energy Society General Meeting (PESGM) 2020 IEEE Power Energy Society General Meeting (PESGM)* pp 1–5
- [14] Yang H 2019 Effects of Aging and Temperature on Supercapacitor Peukert Constant 2019 *IEEE 7th Workshop on Wide Bandgap Power Devices and Applications (WiPDA) 2019 IEEE 7th Workshop on Wide Bandgap Power Devices and Applications (WiPDA)* pp 349–53
- [15] Zheng F, Li Y and Wang X 2018 Study on effects of applied current and voltage on the ageing of supercapacitors *Electrochimica Acta* **276** 343–51
- [16] Xiong G, Kundu A and Fisher T S 2015 Influence of Temperature on Supercapacitor Performance *Thermal Effects in Supercapacitors SpringerBriefs in Applied Sciences and Technology* (Cham: Springer International Publishing) pp 71–114
- [17] Ruiz V, Huynh T, R. Sivakkumar S and G. Pandolfo A 2012 Ionic liquid – solvent mixtures as supercapacitor electrolytes for extreme temperature operation *RSC Advances* **2** 5591–8
- [18] Tan Y B and Lee J-M 2013 Graphene for supercapacitor applications *J. Mater. Chem. A* **1** 14814–43
- [19] Zhang L L, Zhou R and Zhao X S 2010 Graphene-based materials as supercapacitor electrodes *J. Mater. Chem.* **20** 5983–92
- [20] Snook G A, Kao P and Best A S 2011 Conducting-polymer-based supercapacitor devices and electrodes *Journal of Power Sources* **196** 1–12
- [21] Choudhary N, Li C, Moore J, Nagaiah N, Zhai L, Jung Y and Thomas J 2017 Asymmetric Supercapacitor Electrodes and Devices *Advanced Materials* **29** 1605336
- [22] Salanne M, Rotenberg B, Naoi K, Kaneko K, Taberna P-L, Grey C P, Dunn B and Simon P 2016 Efficient storage mechanisms for building better supercapacitors *Nature Energy* **1** 1–10
- [23] Ray A, Roy A, Ghosh M, Alberto Ramos-Ramón J, Saha S, Pal U, Bhattacharya S K and Das S 2019 Study on charge storage mechanism in working electrodes fabricated by sol-gel derived spinel NiMn<sub>2</sub>O<sub>4</sub> nanoparticles for supercapacitor application *Applied Surface Science* **463** 513–25
- [24] Yu Z, Tetard L, Zhai L and Thomas J 2015 Supercapacitor electrode materials: nanostructures from 0 to 3 dimensions *Energy Environ. Sci.* **8** 702–30
- [25] Zhang X, Chang X, Shen Y and Xiang Y 2017 Electrochemical-electrical-thermal modeling of a pouch-type lithium ion battery: An application to optimize temperature distribution *Journal of Energy Storage* **11** 249–57
- [26] Wu B, Li Z and Zhang J 2015 Thermal Design for the Pouch-Type Large-Format Lithium-Ion Batteries: I. Thermo-Electrical Modeling and Origins of Temperature Non-Uniformity *J. Electrochem. Soc.* **162** A181–91
- [27] Goutam S, Nikolian A, Jaguemont J, Smekens J, Omar N, Van Dan Bossche P and Van Mierlo J 2017 Three-dimensional electro-thermal model of li-ion pouch cell: Analysis and comparison of cell design factors and model assumptions *Applied Thermal Engineering* **126** 796–808
- [28] Rani M F H, Razlan Z M, Shahriman A B, Ibrahim Z and Wan W K 2020 Comparative study of surface temperature of lithium-ion polymer cells at different discharging rates by infrared thermography and thermocouple *International Journal of Heat and Mass Transfer* **153** 119595
- [29] Martiny N, Rheinfeld A, Geder J, Wang Y, Kraus W and Jossen A 2014 Development of an All Kapton-Based Thin-Film Thermocouple Matrix for In Situ Temperature Measurement in a Lithium Ion Pouch Cell *IEEE Sensors Journal* **14** 3377–84
- [30] Mutyala M S K, Zhao J, Li J, Pan H, Yuan C and Li X 2014 In-situ temperature measurement in lithium ion battery by transferable flexible thin film thermocouples *Journal of Power Sources* **260** 43–9
- [31] Ghannoum A, Iyer K, Nieva P and Khajepour A 2016 Fiber optic monitoring of lithium-ion batteries: A novel tool to understand the lithiation of batteries 2016 *IEEE SENSORS 2016 IEEE SENSORS* pp 1–3
- [32] Hedman J, Nilebo D, Langhammer E L and Björefors F 2020 Fibre Optic Sensor for Characterisation of Lithium-Ion Batteries *ChemSusChem* **13** 5731–9
- [33] Brice I, Viter R, Draguns K, Grundsteins K, Atvars A, Alnis J, Coy E and Iatsunskyi I 2020 Whispering gallery mode resonators covered by a ZnO nanolayer *Optik* **219** 165296
- [34] Myndrul V, Coy E, Bechelany M and Iatsunskyi I 2021 Photoluminescence label-free immunosensor for the detection of Aflatoxin B1 using polyacrylonitrile/zinc oxide nanofibers *Materials Science and Engineering: C* **118** 111401
- [35] Listewnik P, Hirsch M, Struk P, Weber M, Bechelany M and Jędrzejewska-Szczerska M 2019 Preparation and Characterization of Microsphere ZnO ALD Coating Dedicated for the Fiber-Optic Refractive Index Sensor *Nanomaterials* **9** 306
- [36] Hirsch M, Listewnik P, Struk P, Weber M, Bechelany M and Szczerska M 2019 ZnO coated fiber optic microsphere sensor for the enhanced refractive index sensing *Sensors and Actuators A: Physical* **298** 111594

- [37] Listewnik P, Bechelany M, Jasinski J B and Szczerska M 2020 ZnO ALD-Coated Microsphere-Based Sensors for Temperature Measurements *Sensors* **20** 4689
- [38] Bogdanowicz R, Dettlaff A, Skiba F, Trzcinski K, Szkoda M, Sobaszek M, Ficek M, Dec B, Macewicz L, Wyrębski K, Pasciak G, Geng D, Ignaczak A and Ryl J 2020 Enhanced Charge Storage Mechanism and Long-Term Cycling Stability in Diamondized Titania Nanocomposite Supercapacitors Operating in Aqueous Electrolytes *J. Phys. Chem. C* **124** 15698–712